CLINICAL STUDY

Intra-Left Ventricular Hemodynamics Assessed with 4D Flow Magnetic Resonance Imaging in Patients with Left Ventricular Thrombus

Tomoaki Sakakibara,[1] MD, Kenichiro Suwa,[1] MD, Takasuke Ushio,[2] MD, Tetsuya Wakayama,[3] PhD, Marcus Alley,[4] PhD, Masao Saotome,[1] MD, Hiroshi Satoh,[5] MD and Yuichiro Maekawa,[1] MD

Summary

Left ventricular thrombus (LVT) has been identified to be crucial in patients with reduced ejection fraction (EF). Three-dimensional cine phase-contrast magnetic resonance imaging (4D flow MRI) can visualize the intra-LV vortex during diastole and quantify the maximum flow velocity (Vmax) at the apex. In this study, we investigated whether the change in the intra-LV vortex was associated with the presence of LVT in patients with cardiac disease.

In total, 36 patients (63.5 ± 11.9 years, 28 men, 12/24 with/without LVT) with diffuse LV dysfunction underwent 4D flow MRI. The relative vortex area using streamline images and Vmax of blood flow toward the apex at the apical left ventricle were evaluated. The correlation between the relative vortex area and Vmax was assessed using Pearson's correlation coefficient. The ability to detect LVT was evaluated using the area under the curve (AUC) of the receiver operating characteristic.

The relative vortex area was found to be smaller (27 ± 10% versus 45 ± 11%, $P = 0.000026$), whereas Vmax at the apical left ventricle was lower (19.1 ± 4.4 cm/second versus 27.4 ± 8.9 cm/second, $P = 0.0006$) in patients with LVT. Vmax at the apical left ventricle demonstrated significant correlations with the relative vortex area ($r = 0.43$, $P = 0.01$) and relative transverse length of the vortex ($r = 0.45$, $P = 0.007$). The AUC was 0.91 for the relative vortex area, whereas it was 0.80 for Vmax in the apical left ventricle.

A smaller LV vortex and lower flow velocity at the LV apex were associated with LVT in patients with reduced EF.

(Int Heart J 2021; 62: 1287-1296)

Key words: Three-dimensional cine phase-contrast magnetic resonance imaging, Late gadolinium enhancement, Diffuse left ventricular dysfunction, Ischemic cardiomyopathy, Non-ischemic cardiomyopathy, Flow velocity, Vortex

The presence of left ventricular thrombus (LVT) has been identified to be a critical complication of myocardial infarction (MI) or severe cardiomyopathy, as it can increase the risk of thromboembolic events.[1)] In previous studies, although the incidence of LVT regardless of the underlying heart disease was 0.07%,[2)] the incidence of LVT in patients with MI was 3.5%-8.8% in the percutaneous coronary intervention era,[3-6)] while that in patients with dilated cardiomyopathy was 11%-44%.[7-9)] Thrombus formation in the ventricle is precipitated by reduced wall motion and stasis of blood flow, local myocardial injury, and hypercoagulability, commonly known as the Virchow's triad.[10)] Abnormal LV apical flow is the most crucial factor in predicting LVT development.[11,12)] However, with conventional echocardiography, it is difficult to describe the complex three-dimensional (3D) intracavity blood flow in the left ventricle in patients with cardiac dysfunction complicated by LVT. Three-dimensional cine phase-contrast magnetic resonance imaging (4D flow MRI) is a reliable tool for visualizing and quantifying flow features in the heart and the great vessels.[13)] The spatial 3D vortex of the left ventricle during the diastolic phase can be described using 4D flow MRI.[14-16)] The characteristic features of the intra-LV vortex differed between patients with preserved and those with impaired LV function.[11)] However, only a few studies which examined the flow analysis using two-dimensional echocardiography have elucidated the differences in terms of flow characteristics of the left ventricle between patients with and without LVT.[11,12,17)] Hence, this study aimed

From the [1]Division of Cardiology, Internal Medicine 3, Hamamatsu University School of Medicine, Hamamatsu, Japan, [2]Department of Radiology, Hamamatsu University School of Medicine, Hamamatsu, Japan, [3]Applied Science Laboratory Asia Pacific, GE Healthcare Japan, Tokyo, Japan, [4]Division of Radiology, Stanford University School of Medicine, Stanford, USA and [5]Department of Cardiology, Fujinomiya City General Hospital, Fujinomiya, Japan.

This study was supported by the Ministry of Education, Science, Sports and Culture of Japan, Grants-in-Aid for Scientific Research (Grant Number 20277353 [KS]).

Address for correspondence: Kenichiro Suwa, MD, Division of Cardiology, Internal Medicine 3, Hamamatsu University School of Medicine, 1-20-1 Handayama, Higashi-ku, Hamamatsu 431-3125, Japan. E-mail: wapswing@gmail.com or k-suwa@hama-med.ac.jp

Received for publication December 12, 2020. Revised and accepted July 5, 2021.

doi: 10.1536/ihj.20-792

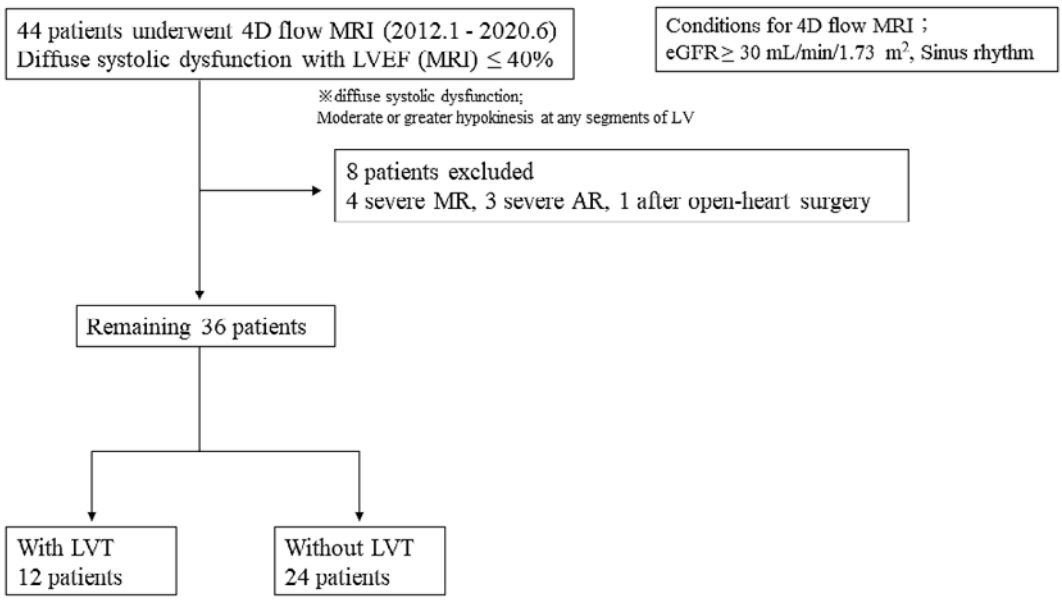

Figure 1. Patient recruitment. Of the 390 patients who underwent 4D flow MRI, 44 with diffuse systolic dysfunction were selected. After excluding 8 patients with contraindications, the remaining 36 patients were divided into 2 groups, that is, the LVT group and the non-LVT group, respectively. MRI indicates magnetic resonance imaging; and LVT, left ventricular thrombus.

to examine the characteristics of intra-LV vortex and flow velocity in patients with severe LV dysfunction with LVT and those without LVT using 4D flow MRI.

Methods

As described in Figure 1, of the patients who met the criteria for contrast-enhanced MRI with an estimated glomerular filtration rate of more than 30 mL/minute/1.73 cm^2, with sinus rhythm (as baseline heart rhythm), and who underwent cardiac MRI including 4D flow MRI and transthoracic echocardiography (TTE) from January 2012 to June 2020 at our institution, a total of 44 patients with various types of cardiac disease and with diffuse hypokinesis and global ejection fraction (EF) of ≤ 40% by cardiac MRI were retrospectively selected for this study. Patients with moderate or greater aortic valve regurgitation (n = 3) and mitral valve regurgitation (n = 4) by TTE and those who underwent any type of open-heart surgery other than coronary artery bypass grafting (n = 1) were excluded from the analysis. The screening for LVT was performed via initial TTE and confirmed by cardiac MRI within a month. In brief, all LVTs were detected incidentally without systemic embolism by initial TTE in 10 patients (83.3%) and eventually by cardiac MRI in two patients (16.7%). Finally, 36 patients were enrolled in this study (63.5 ± 11.9 years, 28 men); they were then divided into two groups, comprising 12 patients with LVT and 24 without LVT. Thromboembolic events were identified based on symptoms and TTE with LVT during the follow-up period. The study protocol was conducted in accordance with the Declaration of Helsinki and was approved by the institutional review board. All study participants provided informed consent accordingly.

All patients underwent TTE for the assessment of cardiac function and size and the detection of LVT. The procedure was performed by experienced sonographers using a commercially available echo system (iE33, Philips Medical Systems, Andover, USA). LV inflow at early diastole (E) and atrial contraction (A), E/A, deceleration time (DcT) on pulsed wave Doppler, and LV septal tissue velocity at early diastole (E') on tissue Doppler were measured in the apical 4-chamber view.

All patients underwent cardiac MRI examinations using a 3T MR scanner (Discovery MR750, GE Healthcare, Waukesha, USA), with a maximum gradient strength of 50 mT/m and a maximum slew rate of 200 mT/m/ms with a commercially available 12-channel phased array body coil.[18] Conventional cardiac MRI including two-dimensional (2D) fast imaging employing steady-state acquisition (FIESTA) and late gadolinium enhancement (LGE) images were acquired in the short, vertical long, and horizontal long axis orientations. The slice thickness/gap was typically 10 mm/0 mm (6-9 slices). 2D-FIESTA cine images were based on the steady-state free precession sequence, and LGE images were based on the inversion recovery prepared by fast gradient echo sequence. A bolus injection of 0.1 mmol/kg gadolinium chelate gadobutrol (Gadovist, Bayer AG, Berlin, Germany) was administered at an injection rate of 2.0 mL/second, followed by 20 mL of saline at the same injection rate. A power injector (Sonic Shot GX, Nemoto Kyorindo Co., Tokyo, Japan) was used for the injection. LV end-diastolic and systolic volume index (LVEDVI and LVESVI), LV stroke volume index (LVSVI), LVEF, and LV mass index (LVMI) were measured using 2D FIESTA, while the prevalence of LGE, a fraction of LGE to LV mass (%LGE) by manual thresholding technique, and the prevalence of apical LGE

were assessed by LGE imaging using Cardiac VX (GE Healthcare, Waukesha, USA).

The 4D flow MRI was performed with full volumetric coverage of the whole heart during free-breathing. The imaging parameters used for coronal 3D Fourier transform (3DFT) fast spoiled gradient echo (FSPGR)-based 4D flow MRI were as follows: TR (ms)/TE (ms)/FA (degree)/NEX of 4.5-5.0/2.0/15/1; field of view (FOV), 32 cm; matrix, 224 × 224; 2 mm thickness, 60 partitions; 20 phases during one cardiac cycle; velocity encoding (VENC) of 200 cm/s; and receiver bandwidth (RBW) of 83.3 kH. Respiratory compensated retrospective cardiac gating was also used in combination with the above-mentioned parameters. The resulting approximate imaging time was 10 minutes, with a reduction factor of 2 for auto-calibrating reconstruction for Cartesian (ARC) sampling.[19] The raw data of 4D flow MRI were transferred to a personal computer (Intel Xeon E3-1270 [3.4 GHz/quad-core] DDR3, 16 GB ECC, Linux) and reconstructed since geometric information for 4D flow MRI, multiphase contrast-enhanced 3D FSPGR MR angiography (MRA) was performed before LGE imaging. The imaging parameters for coronal 3 D FSPGR MRA were as follows: TR (ms)/TE (ms)/FA (degree)/NEX of 2.7/1.0/12/1, FOV of 32 cm, size of the reconstructed matrix with the aid of zero-fill interpolation processing of 224 × 224, RBW of 83.3 kHz, and imaging time of 33 sec for four phases.

For post-processing, 3D phase contrast and MRA datasets were formatted in Digital Imaging and Communications in Medicine format and analyzed using the software Flova (R'-Tech Co., Hamamatsu, Japan), as described elsewhere.[20] We then selected the region of interest, including the left atrium and left ventricle, for 4D flow MRI. Segmentation was performed for the heart and vascular wall structures using the 3D MRA datasets for the peak of the R wave with MRA images for 4D flow MRI using the region growing method. The shapes were also created using the marching cubes method and then edited manually.

To identify the intra-LV flow patterns, 3D visualization was performed using Flova software. The 3D flow information was interpolated with a spatial resolution of 2 × 2 × 2 mm using 3D datasets. To generate 3D streamline images using the Runge-Kutta method, we manually set the emitter planes traversing the basal, mid, and apical areas of the LV. The overall post-processing time was approximately 60 minutes. We then evaluated the presence, position, shape, and size of the late diastolic vortex in the LV. The intra-LV vortex was defined as concentric circles using streamline images.

The location of the late-diastolic intra-LV vortex core and the size of the vortex were analyzed on the basis of the image obtained from the left lateral view of the LV. The location of the vortex core was evaluated on combined streamline and 3D MRA images by calculating the distance from the atrioventricular junction to the center of the vortex, which was expressed as the absolute value (mm) or relative ratio (%) to the longitudinal length of the LV. The maximum longitudinal and transverse lengths and the maximum area of the vortex were measured as absolute values (mm or cm^2) and relative ratios (%) to those of the LV. The sphericity indices of the left ventricle and vortex were calculated by dividing the maximum longitudinal lengths by their maximum transverse lengths.[14]

Intra-LV blood flow velocity was measured using 4D flow MRI. Three analysis planes were then set manually across the center of the basal, mid, and apical areas of the left ventricle perpendicular to the long axis at late diastole. Peak velocity (Vmax) at each anatomical location in the left ventricle was quantified bi-directionally, that is, toward the apex and base.

The entire 4D flow MRI analysis, including segmentation of the heart and vessel walls, setting the analysis planes, and evaluating hemodynamics, was repeated in all patients by a blinded observer (KS) for the assessment of interobserver variabilities.

Continuous data are expressed as mean ± standard deviation or as medians with interquartile ranges. Categorical data are presented as numbers and percentages. Continuous variables were compared using the two-sided unpaired t-test or Mann-Whitney *U*-test. Categorical variables were compared using the Fisher's exact test. The inter- and intra-observer variabilities for the determination of the presence of intra-LV vortex and hemodynamic features given by 4D flow MRI were evaluated by calculating Cohen's kappa (κ) coefficient or intraclass correlation coefficients (ICC). The correlations between the vortex size parameters and Vmax were assessed using the Pearson's correlation coefficient. The ability to detect LVT using 4D flow MRI-derived parameters was assessed using receiver operating characteristic (ROC) analysis. Statistical significance was set at $P < 0.05$. All statistical analyses were performed using a statistical software package (EZR v1.40).

Results

As summarized in Table I, no significant difference was observed between the LVT group (60.4 ± 11.4 years) and non-LVT group (65.4 ± 12.2 years, $P = 0.25$) in terms of age. No significant difference was also noted in the proportion of patients classified according to the New York Heart Association (NYHA) functional classification between the two groups ($P = 0.41$). As an etiology of cardiomyopathy, the incidence of ischemic cardiomyopathy (ICM) did not vary between the two groups (66.7% in the LVT group versus 41.7% in the non-LVT group, $P = 0.29$). In the LVT group, two patients had a subacute phase of MI (days 11 and 17 from onset). From the patients in the non-ischemic cardiomyopathy (NICM) group, two patients with dilated cardiomyopathy (DCM), one patient with end-stage hypertrophic cardiomyopathy (HCM), and one patient with cardiac sarcoidosis were included in the LVT group, while 13 patients with DCM and one with drug-induced cardiomyopathy were included in the non-LVT group, respectively. All patients with LVT developed a thrombus in the apex, except for one patient with NICM who developed LVT in the posterolateral area. The size of the LVT was 1.1 (0.74-2.05) cm^3. There were no significant differences between the two groups in terms of underlying diseases and medications. Moreover, two patients from the LVT group (16.7%) and six from the non-LVT

Table I. Patient Characteristics

	LVT (n = 12)	Non-LVT (n = 24)	P-value
Age, years	60.4 ± 11.4	65.4 ± 12.2	0.25
Male, n (%)	9 (91.7%)	19 (79.2%)	0.64
BSA, m^2	1.73 ± 0.20	1.63 ± 0.18	0.15
BMI	23.4 ± 4.2	22.6 ± 3.9	0.58
NYHA (I/II/III/IV), n	8/13/3/0	3/5/3/1	0.41
ICM, n (%)	8 (66.7%)	10 (41.7%)	0.29
Non-ICM, n (%)	4 (33.3%)	14 (58.3%)	0.29
DCM, n	2	13	
End-stage HCM, n	1	0	
Sarcoidosis, n	1	0	
Drug-induced, n	0	1	
Smoking, n (%)	4 (33.3%)	8 (33.3%)	1.00
Comorbidity			
DM	2 (16.7%)	10 (41.7%)	0.26
CKD (eGFR < 60), n (%)	7 (58.3%)	17 (70.8%)	0.48
HT, n (%)	3 (25.0%)	8 (33.3%)	0.72
HL, n (%)	6 (50.0%)	13 (54.2%)	1.00
Stroke, n (%)	1 (8.3%)	2 (8.3%)	1.00
Medications			
Diuretics, n (%)	5 (41.7%)	16 (66.7%)	0.18
Beta-blockers, n (%)	7 (58.3%)	16 (66.7%)	0.72
ACE-Is/ARBs, n (%)	6 (50.0%)	18 (75.0%)	0.16
Statins, n (%)	5 (41.7%)	13 (54.2%)	0.73
Anticoagulants, n (%)	2 (16.7%)	6 (25.0%)	0.69
Antiplatelet agents, n (%)	6 (50.0%)	13 (54.2%)	1.00
TTE			
E, cm/second	57.2 ± 21.4	77.0 ± 26.8	0.033
A, cm/second	59.8 ± 20.4	67.3 ± 31.5	0.46
E/A	1.2 ± 0.8	1.6 ± 1.2	0.28
DcT, ms	202.3 ± 91.2	175.1 ± 65.8	0.33
E', cm/second	3.6 ± 1.2	5.4 ± 2.0	0.0086
E/E'	16.8 ± 7.7	15.4 ± 5.3	0.52

Values are mean ± SD, n, or n (%). A indicates left ventricular inflow at atrial contraction; ACE-Is, angiotensin-converting enzyme inhibitors; ARBs, angiotensin receptor blockers; BSA, body surface area; BMI, body mass index; CKD, chronic kidney disease; DCM, dilated cardiomyopathy; DcT, deceleration time on pulsed wave Doppler; DM, diabetes mellitus; E, left ventricular inflow at early diastole; E', LV septal tissue velocity at early diastole on tissue Doppler; eGFR, estimated glomerular filtration rate; HCM, hypertrophic cardiomyopathy; HT, hypertension; HL, hyperlipidemia; ICM, ischemic cardiomyopathy; LVT, left ventricular thrombus; and NYHA, New York Heart Association functional class.

group (25.0%) were taking anticoagulants as treatment for paroxysmal atrial fibrillation. After the diagnosis, of LVT, all patients in the LVT group were immediately started on warfarin therapy, and they continued the same. None of the patients were treated with additional anticoagulant agents for other reasons. None of the patients in the entire cohort experienced systemic embolism during the follow-up period (54.5 [31.5-80.0] months in LVT group and 25.5 [9.75-74.0] months in the non-LVT group). Two patients in the non-LVT group died on account of end-stage heart failure. E and E' in the LVT group were noted to be significantly smaller than those in the non-LVT group (E: 57.2 ± 21.4 cm/second versus 77.0 ± 26.8 cm/second; P = 0.033, E': 3.6 ± 1.2 cm/second versus 5.4 ± 2.0 cm/second; P = 0.0086).

On cardiac MRI, LVSVI was significantly smaller in the LVT group (26.2 ± 5.5 mL/m^2 versus 31.5 ± 9.8 mL/m^2, P = 0.044), while LVEDVI, LVESVI, and LVEF were not different between groups (Table II). LGE appeared in most patients (all patients in the LVT group and 83.3% of the patients in the non-LVT group). %LGE did not differ between LVT group and non-LVT group even in the sub-cohort only with ICM (Table II and Table III). The prevalence of apical LGE was significantly high in the LVT group than that in non-LVT group (83.3% versus 45.8%, P = 0.040) in the entire cohort, while it was noted to not vary between LVT and non-LVT groups in the sub-cohort only with ICM.

A clockwise-directional intra-LV vortex flow in the left lateral view of the left ventricle was observed in all patients in the late diastolic phase by 4D flow MRI streamline image (Figure 2). The inter- and intra-observer variability for the determination of the presence of an intra-LV vortex was perfect (κ = 1 for both). The LV vor-

Table II. Conventional Cardiac Magnetic Resonance and LV Size and Blood Flow Features in LV by 4D Flow MRI in the Entire Cohort

	LVT (n = 12)	Non-LVT (n = 24)	P-value
Cine			
HR, beat/minute	67 ± 14	66 ± 18	0.85
LVEDVI, mL/m^2	116.2 ± 51.0	127.7 ± 46.4	0.50
LVESVI, mL/m^2	90.1 ± 49.1	96.2 ± 39.4	0.69
LVSVI, mL/m^2	26.2 ± 5.5	31.5 ± 9.8	0.044
LVEF, %	26.0 ± 9.6	25.6 ± 5.8	0.91
LVMI, g/m^2	101.1 ± 32.5	91.5 ± 33.4	0.43
LGE, n (%)	12 (100%)	20 (83.3%)	0.28
LGE in ICM, n (%)	8 (66.7%)	10 (41.6%)	0.29
LGE in NICM, n (%)	4 (33.3%)	10 (41.6%)	0.73
%LGE, %	23.3 ± 13.7	19.7 ± 13.8	0.46
Apical LGE, n (%)	10 (83.3%)	11 (45.8%)	0.040
LV size			
Longitudinal length of LV, mm	96.8 ± 10.6	93.7 ± 6.3	0.37
Transverse length of LV, mm	64.9 ± 12.0	66.7 ± 9.4	0.62
Sphericity index of LV, %	152 ± 22	142 ± 16	0.14
LV area, cm^2	54.0 ± 14.1	52.4 ± 12.2	0.73
Vortex size			
Longitudinal length of vortex, mm	56.1 ± 14.9	69.4 ± 10.9	0.0045
Transverse length of vortex, mm	33.5 ± 8.2	45.3 ± 10.3	0.0015
Sphericity index of vortex, %	172 ± 55	157 ± 26	0.38
Vortex area, cm^2	14.5 ± 6.4	23.8 ± 8.1	0.0013
Relative vortex size			
Relative longitudinal length of vortex, %	55 ± 14	70 ± 10	0.00064
Relative transverse length of vortex, %	51 ± 11	67 ± 10	0.000059
Relative vortex area, %	27 ± 10	45 ± 11	0.000026
Vortex location			
Distance to vortex core, mm	33.0 ± 6.9	41.7 ± 10.5	0.014
Relative distance to vortex core, %	32 ± 6	42 ± 8	0.00098
Vmax toward apex			
At basal LV, cm/second	54.2 ± 13.6	54.0 ± 18.3	0.98
At mid LV, cm/second	30.7 ± 7.66	40.6 ± 6.4	0.019
At apical LV, cm/second	19.1 ± 4.4	27.4 ± 8.9	0.00060
Vmax toward base			
At basal LV, cm/second	40.8 ± 14.2	40.2 ± 9.3	0.89
At mid LV, cm/second	23.0 ± 9.0	31.1 ± 10.1	0.024
At apical LV, cm/second	16.1 ± 9.6	23.3 ± 7.6	0.020

Values are mean ± SD and number (%). Sphericity index: longitudinal length/transverse length. The relative vortex sizes were calculated as the vortex length or area divided by the corresponding LV length or area. The relative value of the distance to the vortex core from the AV junction was calculated by dividing its absolute value by the LV longitudinal length. EDVI, end-diastolic volume index; ESVI, end-systolic volume index; HR, heart rate; ICM, ischemic cardiomyopathy; LGE, late gadolinium enhancement; LV, left ventricular; LVEF, left ventricular ejection fraction; LVMI, left ventricular mass index; LVT, left ventricular thrombus; NICM, non-ischemic cardiomyopathy; SVI, stroke volume index; Vmax, maximum flow velocity.

tex flow characteristics are presented in Table II. The relative longitudinal length (55 ± 14% versus 70 ± 10%, P = 0.00064), relative transverse length of the vortex (51 ± 11% versus 67 ± 10%, P = 0.000059), and relative vortex area (27 ± 10% versus 45 ± 11%, P = 0.000026) in the LVT group were significantly smaller than those in the non-LVT group. The relative distance to the vortex core in the LVT group was shorter than that in the non-LVT group (32 ± 6% versus 42 ± 8%, P = 0.00098). The inter- and intra-observer agreement for the relative vortex size included the relative longitudinal length of the vortex (ICC = 0.88, 0.98), relative transverse length of vortex (ICC = 0.94, 0.98), relative vortex area (ICC = 0.88, 0.98), and the relative distance to the vortex core (ICC = 0.96, 0.97).

The Vmax at each anatomical location of the left ventricle is summarized in Figure 3. The Vmax of blood flow in the apical area of the left ventricle toward the apex and the base were significantly lower in the LVT group than in the non-LVT group (toward the apex: 19.1 ± 4.4 cm/second versus 27.4 ± 8.9 cm/second; P = 0.00060, toward the base: 16.1 ± 9.6 cm/second versus 23.3 ± 7.6 cm/second; P = 0.020). The inter- and intra-observer variability for Vmax (ICC = 0.81, 0.95) were deemed excellent.

As summarized in Table III, in sub-cohort only with

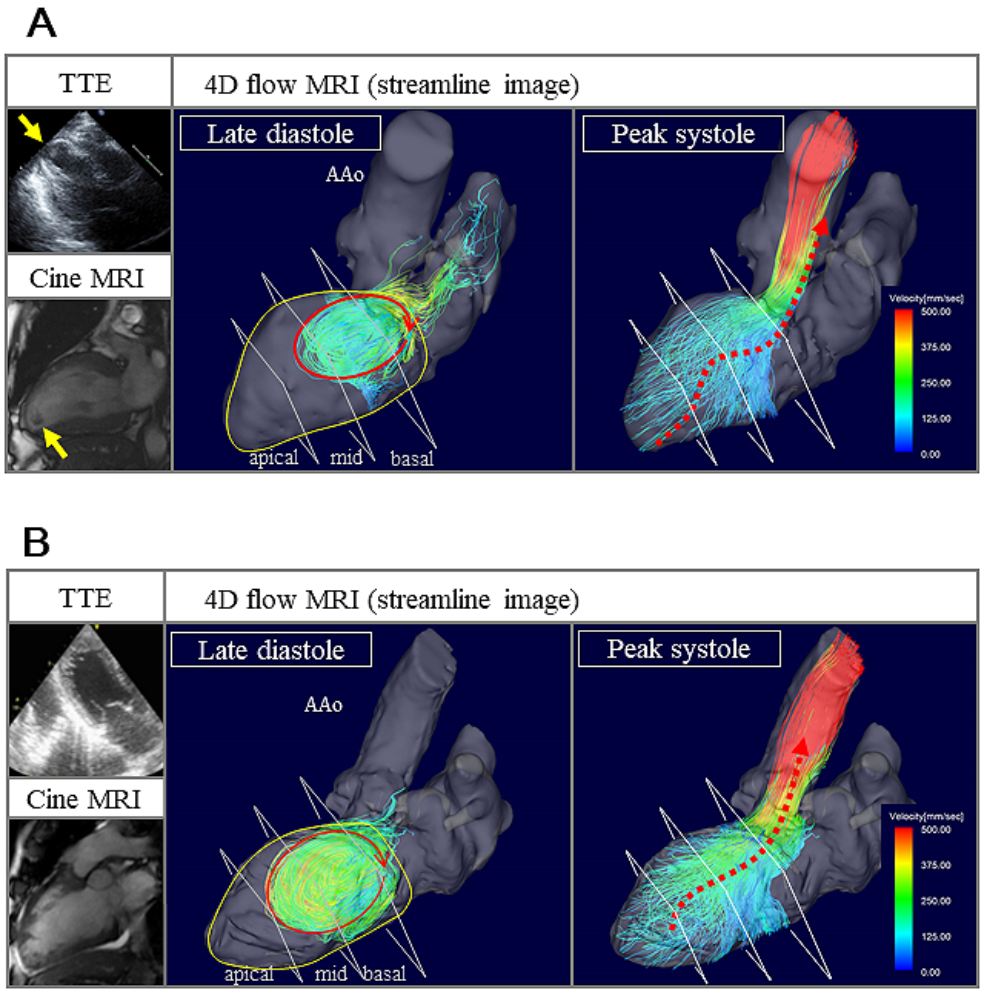

Figure 2. Transthoracic echocardiography images, cine MRI scans, and streamline images obtained by 4D flow MRI. Imaging scans of patients with LVT (**A**) and without LVT (**B**) are presented. LVTs were detected by TTE and cine MRI (yellow arrows). Four-dimensional flow MRI exhibited clockwise directional vortex flow in late diastole in both cases (solid red circles with arrows). Non-vortical ejection flow during peak systole was observed in both cases (broken red arrows). The absolute vortex area (solid red circles with arrows), LV area (yellow circles), and the flow velocities toward the apex and base were measured in three analysis planes set in the apical, mid, and basal areas of the left ventricle. MRI indicates magnetic resonance imaging; LVT, left ventricular thrombus; and TTE, transthoracic echocardiogram.

ICM, the relative longitudinal length (54 ± 15% versus 69 ± 12%, $P = 0.033$), the relative transverse length of the vortex (49 ± 11% versus 66 ± 13%, $P = 0.010$), and the relative vortex area (25 ± 9% versus 43 ± 15%, $P = 0.0095$) in the LVT group were significantly smaller than that in the non-LVT group. The Vmax of blood flow in the apical area of the left ventricle toward the apex and the base were significantly lower in the LVT group than in the non-LVT group (toward the apex: 18.8 ± 3.5 cm/second versus 25.7 ± 7.9 cm/second; $P = 0.027$, toward the base: 16.9 ± 10.2 cm/second versus 20.2 ± 7.6 cm/second; $P = 0.045$).

As shown in Figure 3, the Vmax of blood flow toward the apex in the apical area of the left ventricle demonstrated significant correlations with relative vortex area ($r = 0.43$, $P = 0.001$) and with relative transverse length of vortex ($r = 0.45$, $P = 0.007$). Although not significant, a positive correlation was observed between Vmax toward the apex in the apical left ventricle and relative longitudinal length of the vortex ($r = 0.29$, $P = 0.08$). The relative distance to the vortex core demonstrated no correlation with Vmax toward both directions and any locations of the LV.

The ROC analysis for the detection of LVT revealed that areas under the curves were 0.91 for the relative vortex area (Figure 4A) and 0.80 for Vmax toward the apex in the apical left ventricle (Figure 4B). The best cut-off values were ≤ 34.7% (sensitivity 0.917, specificity 0.833) for relative vortex area and ≤ 22.2 cm/second (sensitivity 0.833 and specificity 0.708) for Vmax toward the apex in the apical LV.

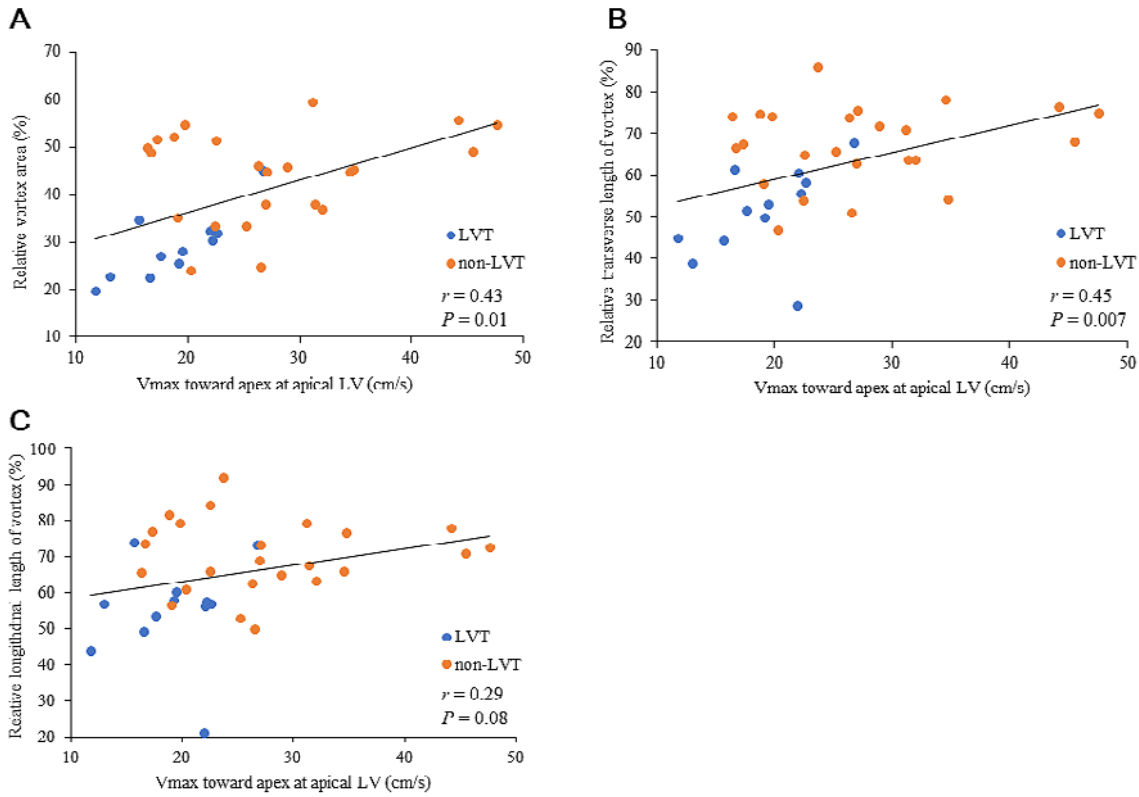

Figure 3. Association between vortex size and Vmax. Significant moderate correlations were observed between Vmax toward apex at the apical left ventricle and relative vortex area (**A**, $r = 0.49$, $P = 0.007$), and between Vmax toward apex at the apical left ventricle and relative transverse length of vortex (**B**, $r = 0.51$, $P = 0.004$). There was a trend toward a correlation between Vmax toward apex at the apical left ventricle and relative longitudinal length of vortex (**C**, $r = 0.35$, $P = 0.064$). Vmax indicates maximum flow velocity.

Discussion

In this study, we have examined the relationship between LVT and intra-LV vortex formation during the diastolic phase, which was observed in all patients using 4D flow MRI streamline images. The main findings of this study were as follows: (1) although there were no differences in the LVEDVI, LVEF, and sphericity index of the left ventricle determined by cardiac MRI between the LVT and non-LVT groups, the relative vortex area was smaller, and the relative distance to the vortex core was shorter in the LVT group; (2) the Vmax toward the apex measured in the apical area of the left ventricle was significantly smaller in the LVT group; and (3) Vmax toward the apex measured in the apical area of the left ventricle demonstrated significant correlations with relative vortex area and relative transverse length of the vortex.

As described previously, Virchow's triad, that is, blood flow, blood composition, and vascular function, is the most critical pathophysiological mechanism in thrombogenesis.[21] Blood stasis due to poor myocardial contraction, myocardial injury, and hypercoagulability are known risk factors for LVT.[10] However, previous studies have mainly focused on the causes of reduced ventricular contractility instead of assessing intra-LV blood flow. Nowadays, using 4D flow MRI sequences, blood flow can be visualized and quantified in various parts of the cardiovascular system.[14,20,22,23] As a surrogate marker of stasis in the left ventricle, we have evaluated Vmax in the base, mid, and apical areas of the LV. The decreased Vmax in the apical area of the left ventricle in the LVT group indicated stasis of blood flow at the apex.[9] Moreover, there were differences in the vortex size between the LVT and non-LVT groups. We have considered that the relatively smaller LV vortex size led to insufficient blood delivery to the apex, resulting in LVT formation.

In a previous study, ICM was considered a risk factor for LVT.[2] The three components related to LVT formation are stasis caused by regional LV wall akinesia; subendocardial tissue injury and inflammation; and hypercoagulability during acute coronary syndrome.[21] Considering these factors, we did not include patients within 10 days of acute MI in our study. Although the proportion of ICM was relatively high in the LVT group, no statistical difference was noted between the two groups (55.6% versus 30.0%, $P = 0.369$) in our study. Although some previous studies suggested that the sphericity index of the left ventricle can be used as a marker for LV remodeling,[24] which is similar to the findings of Kaolawanich, *et al.*,[25] no association was observed between the sphericity index of the left ventricle and LVT. As per our findings, we were able to determine the higher prevalence of apical LGE in LVT group in the entire cohort, but not in the sub-cohort only with ICM. This finding may indicate the association

Table III. Conventional Cardiac Magnetic Resonance and LV Size and Blood Flow Features in LV by 4D Flow MRI in Sub-cohort Only with ICM

	LVT (n = 8)	Non-LVT (n = 10)	P-value
Cine			
HR, beat/minute	66.1 ± 7.7	69.7 ± 13.9	0.53
LVEDVI, mL/m^2	102.6 ± 49.0	116.1 ± 37.2	0.52
LVESVI, mL/m^2	75.8 ± 44.2	84.5 ± 30.3	0.63
LVSVI, mL/m^2	26.8 ± 6.0	31.6 ± 9.2	0.23
LVEF, %	28.9 ± 7.3	27.8 ± 5.4	0.73
LVMI, g/m^2	84.4 ± 22.1	79.2 ± 33.2	0.72
LGE, n (%)	8 (100%)	10 (100%)	1.0
%LGE, %	24.6 ± 12.5	19.7 ± 13.8	0.46
Apical LGE, n (%)	8 (100%)	9 (90%)	1.0
LV size			
Longitudinal length of LV, mm	96.8 ± 13.2	92.3 ± 7.7	0.38
Transverse length of LV, mm	61.5 ± 8.8	61.0 ± 7.7	0.91
Sphericity index of LV, %	158 ± 11	153 ± 14	0.39
LV area, cm^2	51.8 ± 15.7	50.6 ± 14.2	0.87
Vortex size			
Longitudinal length of vortex, mm	53.1 ± 15.3	66.1 ± 12.2	0.062
Transverse length of vortex, mm	30.9 ± 7.4	40.3 ± 10.4	0.047
Sphericity index of vortex, %	178 ± 67	168 ± 23	0.68
Vortex area, cm^2	12.6 ± 5.2	21.6 ± 8.9	0.018
Relative vortex size			
Relative longitudinal length of vortex, %	54 ± 15	69 ± 12	0.033
Relative transverse length of vortex, %	49 ± 11	66 ± 13	0.010
Relative vortex area, %	25 ± 9	43 ± 15	0.0095
Vortex location			
Distance to vortex core, mm	30.5 ± 6.9	38.5 ± 14.2	0.17
Relative distance to vortex core, %	31 ± 7	39 ± 10	0.051
Vmax toward apex			
At basal LV, cm/second	54.0 ± 10.0	52.5 ± 11.9	0.80
At mid LV, cm/second	29.5 ± 4.7	36.6 ± 8.1	0.047
At apical LV, cm/second	18.8 ± 3.5	25.7 ± 7.9	0.027
Vmax toward base			
At basal LV, cm/second	45.4 ± 14.3	38.6 ± 6.2	0.24
At mid LV, cm/second	23.1 ± 10.8	25.6 ± 6.9	0.57
At apical LV, cm/second	16.9 ± 10.2	20.2 ± 7.6	0.045

Values are mean ± SD and number (%). Sphericity index: longitudinal length/transverse length. The relative vortex sizes were calculated as the vortex length or area divided by the corresponding LV length or area. The relative value of the distance to the vortex core from the AV junction was calculated by dividing its absolute value by the LV longitudinal length. EDVI indicates end-diastolic volume index; ESVI, end-systolic volume index; HR, heart rate; ICM, ischemic cardiomyopathy; LGE, late gadolinium enhancement; LV, left ventricle; LVEF, left ventricular ejection fraction; LVMI, left ventricular mass index; LVT, left ventricular thrombus; SVI, stroke volume index; and Vmax, maximum flow velocity.

between apical LGE in non-ICM and LVT, although more patients with non-ICM are required to confirm.

Harfi, *et al.* determined the E-wave propagation index (EPI), which was calculated as E-wave velocity time-integral (VTI) divided by LV length, by performing an echocardiographic examination, and reported that an EPI of less than 1 is an independent risk predictor of LVT formation.[26] Similar to the findings of this study, our results showed that the E-wave velocity in the LVT group was significantly lower than that in the non-LVT group, suggesting that the strength of LV inflow contributed to the prevention of apical thrombus formation. As the Vmax toward the LV apex in the basal area of the left ventricle was not different between the LVT and non-LVT groups, other factors may have affected the flow between the mitral valve and the basal area of the LV. Although EPI can be instantly and noninvasively calculated, it is an indirect tool for estimating the hemodynamics in the apical area of the LV, and other factors that affect the blood flow from the mitral valve to the apex may be missed. Conversely, as the flow velocities in any part of the LV, including the apex, were measured in a direct manner, 4D flow MRI is a promising tool for evaluating intra-LV hemodynamics, although it generally consumes more time than echocardiography. Although merely speculative, since we did not show the superiority, both EPI by echocardiography and 4D flow MRI may be good options to evaluate the hemodynamics in the apical area of the LV. Pankaj, *et al.* reported that patients with LVT after MI showed a significantly enhanced kinetic energy (KE) decrease from the

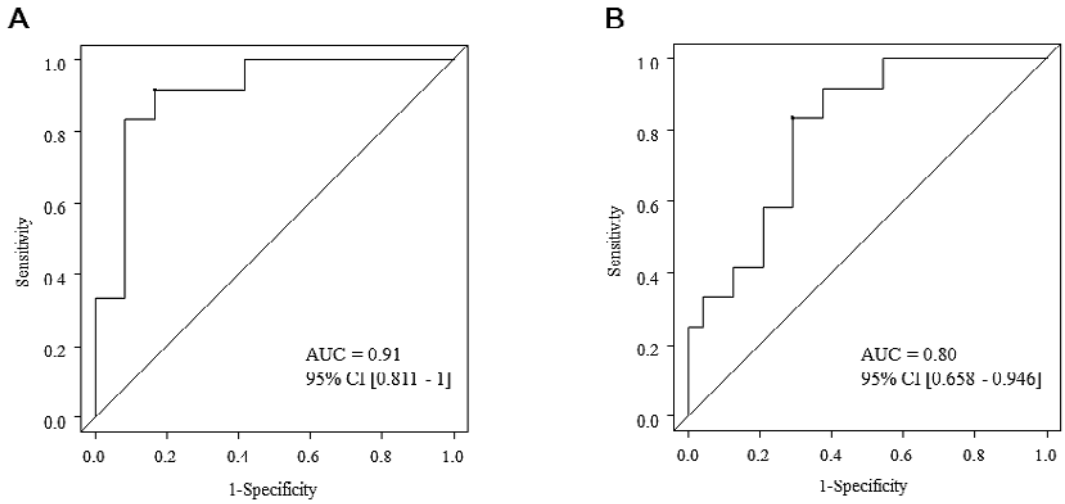

Figure 4. ROC analysis for the detection of LVT by the relative vortex area (**A**) and Vmax toward the apex in the apical LV (**B**). For the relative vortex area (**A**), AUC was 0.91 and the best cut-off value was ≤ 34.7% with sensitivity of 0.917 and specificity of 0.833. For the Vmax toward the apex in the apical LV (**B**), AUC was 0.80 and the best cut-off value was ≤ 22.2 cm/second with sensitivity of 0.833 and specificity of 0.708. AUC indicates area under the curve; CI, confidential interval; LV, left ventricle; LVT, left ventricular thrombus; and ROC, receiver operating characteristic.

basal to the apical areas of the LV.[27] We measured the simple blood flow velocity instead of the KE decrease, which is the product of the blood density, voxel volume, and velocity magnitude. As the LV morphology and hematocrit were the same between the LVT and non-LVT groups, we expected similar differences between the two groups. In this study, we revealed a significant correlation between vortex size and blood velocity toward the apex in the apical LV. This finding suggested that the larger vortex may have contributed to maintaining a higher blood velocity in the apical LV. In other words, the large vortex in severe LV dysfunction could prevent LVT formation.

This study had some limitations. The small sample size and resulting lack of multivariate analysis were the critical limitation. In order to maintain uniformity in LV morphology between the LVT and non-LVT groups, we excluded patients with asynergic LV wall motion and valvular defects. The exclusion of these patients enabled us to simplify the patient's background. However, this might have caused a bias by affecting intra-LV hemodynamics. Hence, further investigations are needed to assess the hemodynamics in patients with LV asynergy to assess the universality of the parameters related to LVT in this study. The heterogeneous background of impaired LV function (ICM and non-ICM) is another limitation. We could perform sub-cohort analysis only with ICM and ascertain a similar trend of small vortex and slower Vmax, but not in non-ICM sub-cohort because of limited sample size. The shape of the heart and vessels was determined only at the peak of the R-wave, so that the location of the basal, mid, and apical left ventricle was fixed throughout the cardiac phases. The LVT itself might disturb blood flow in the LV. The lack of investigation between hemodynamics at LVT existence and LVT disappearance was a limitation because we had no follow-up 4D flow MRI. However, the effect of LVT on the vortex size and Vmax of blood flow can be neglected because the size of the LVT was considerably small for dilated LV. Furthermore, as the sample size in our study was too small to perform a multivariate analysis, a large-scale longitudinal follow-up study is warranted to evaluate the relationship between hemodynamics and the incidence of LVT. Finally, the stagnant slow flow might have been missed and mixed with the background noise because of the single and relatively high VENC settings in this study. Multiple VENC settings for high and low velocities may overcome this issue in a future study.

In conclusion, a smaller LV vortex and lower flow velocity at the LV apex were associated with LVT in patients with diffuse systolic dysfunction. A large-scale longitudinal follow-up study is warranted to evaluate the diagnostic performance of hemodynamic characteristics using 4D flow MRI to predict LVT formation.

Disclosure

Conflicts of interest: Not applicable.

References

1. Sharma ND, McCullough PA, Philbin EF, Weaver WD. Left ventricular thrombus and subsequent thromboembolism in patients with severe systolic dysfunction. Chest 2000; 117: 314-20.
2. Lee JM, Park JJ, Jung HW, *et al*. Left ventricular thrombus and subsequent thromboembolism, comparison of anticoagulation, surgical removal, and antiplatelet agents. J Atheroscler Thromb 2013; 20: 73-93.
3. Delewi R, Nijveldt R, Hirsch A, *et al*. Left ventricular thrombus formation after acute myocardial infarction as assessed by cardiovascular magnetic resonance imaging. Eur J Radiol 2012; 81: 3900-4.
4. Pöss J, Desch S, Eitel C, de Waha S, Thiele H, Eitel I. Left ven-

tricular thrombus formation after ST-segment-elevation myocardial infarction: Insights from a cardiac magnetic resonance multicenter study. Circ Cardiovasc Imaging 2015; 8: e003417.
5. Sürder D, Gisler V, Corti R, *et al*. Thrombus formation in the left ventricle after large myocardial infarction - Assessment with cardiac magnetic resonance imaging. Swiss Med Wkly 2015; 145: w14122.
6. Weinsaft JW, Kim J, Medicherla CB, *et al*. Echocardiographic algorithm for post-myocardial infarction LV thrombus: A gatekeeper for thrombus evaluation by delayed enhancement CMR. JACC Cardiovasc Imaging 2016; 9: 505-15.
7. Crawford TC, Smith WT 4th, Velazquez EJ, Taylor SM, Jollis JG, Kisslo J. Prognostic usefulness of left ventricular thrombus by echocardiography in dilated cardiomyopathy in predicting stroke, transient ischemic attack, and death. Am J Cardiol 2004; 93: 500-3.
8. Kalaria VG, Passannante MR, Shah T, Modi K, Weisse AB. Effect of mitral regurgitation on left ventricular thrombus formation in dilated cardiomyopathy. Am Heart J 1998; 135: 215-20.
9. Wilensky RL, Jung SC. Thromboembolism in patients with decreased left ventricular function: Incidence, risk, and treatment. J Cardiovasc Risk 1995; 2: 91-6.
10. Habash F, Vallurupalli S. Challenges in management of left ventricular thrombus. Ther Adv Cardiovasc Dis 2017; 11: 203-13.
11. Delemarre BJ, Visser CA, Bot H, Dunning AJ. Prediction of apical thrombus formation in acute myocardial infarction based on left ventricular spatial flow pattern. J Am Coll Cardiol 1990; 15: 355-60.
12. Van Dantzig JM, Delemarre BJ, Bot H, Koster RW, Visser CA. Doppler left ventricular flow pattern versus conventional predictors of left ventricular thrombus after acute myocardial infarction. J Am Coll Cardiol 1995; 25: 1341-6.
13. Markl M, Frydrychowicz A, Kozerke S, Hope M, Wieben O. 4D flow MRI. J Magn Reson Imaging 2012; 36: 1015-36.
14. Suwa K, Saitoh T, Takehara Y, *et al*. Intra-left ventricular flow dynamics in patients with preserved and impaired left ventricular function: Analysis with 3D cine phase contrast MRI (4D-Flow). J Magn Reson Imaging 2016; 44: 1493-503.
15. Ebbers T. Flow imaging: Cardiac applications of 3D cine phase-contrast MRI. Curr Cardiovasc Imaging Rep 2011; 4: 127-33.
16. Elbaz MSM, Calkoen EE, Westenberg JJM, Lelieveldt BPF, Roest AAW, Van Der Geest RJ. Vortex flow during early and late left ventricular filling in normal subjects: Quantitative characterization using retrospectively gated 4D flow cardiovascular magnetic resonance and three-dimensional vortex core analysis. J Cardiovasc Magn Reson 2014; 16: 78.
17. Son JW, Park WJ, Choi JH, *et al*. Abnormal left ventricular vortex flow patterns in association with left ventricular apical thrombus formation in patients with anterior myocardial infarction: A quantitative analysis by contrast echocardiography. Circ J 2012; 76: 2640-6.
18. Matoh F, Satoh H, Shiraki K, *et al*. Usefulness of delayed enhancement magnetic resonance imaging to differentiate dilated phase of hypertrophic cardiomyopathy and dilated cardiomyopathy. J Card Fail 2007; 13: 372-9.
19. Brau ACS, Beatty PJ, Skare S, Bammer R. Comparison of reconstruction accuracy and efficiency among autocalibrating data-driven parallel imaging methods. Magn Reson Med 2008; 59: 382-95.
20. Suwa K, Saitoh T, Takehara Y, *et al*. Characteristics of intra-left atrial flow dynamics and factors affecting formation of the vortex flow: Analysis with phase-resolved 3-dimensional cine phase contrast magnetic resonance imaging. Circ J 2015; 79: 144-52.
21. Wolberg AS, Aleman MM, Leiderman K, Machlus KR. Procoagulant activity in hemostasis and thrombosis: Virchow's triad revisited. Anesth Analg 2012; 114: 275-85.
22. Jung B, Odening KE, Dall'Armellina E, *et al*. A quantitative comparison of regional myocardial motion in mice, rabbits and humans using in-vivo phase contrast CMR. J Cardiovasc Magn Reson 2012; 14: 87.
23. Suwa K, Akita K, Iguchi K, Sugiyama M, Maekawa Y. Improved blood flow after percutaneous transluminal septal myocardial ablation visualized by 4D flow cardiac magnetic resonance in a case of hypertrophic obstructive cardiomyopathy. Eur Heart J Cardiovasc Imaging 2018; 19: 1389.
24. Di Donato M, Dabic P, Castelvecchio S, *et al*. Left ventricular geometry in normal and post-anterior myocardial infarction patients: Sphericity index and "new" conicity index comparisons. Eur J Cardiothorac Surg 2006; 29(Supplement 1): S225-30.
25. Kaolawanich Y, Boonyasirinant T. Usefulness of apical area index to predict left ventricular thrombus in patients with systolic dysfunction: A novel index from cardiac magnetic resonance. BMC Cardiovasc Disord 2019; 19: 15.
26. Harfi TT, Seo JH, Yasir HS, *et al*. The E-wave propagation index (EPI): A novel echocardiographic parameter for prediction of left ventricular thrombus. Derivation from computational fluid dynamic modeling and validation on human subjects. Int J Cardiol 2017; 227: 662-7.
27. Garg P, Van Der Geest RJ, Swoboda PP, *et al*. Left ventricular thrombus formation in myocardial infarction is associated with altered left ventricular blood flow energetics. Eur Heart J Cardiovasc Imaging 2019; 20: 108-17.